High-Ion Temperature Experiments with Negative-Ion-Based NBI in LHD

Y. Takeiri 1), S. Morita 1), K. Tsumori 1), K. Ikeda 1), Y. Oka 1), M. Osakabe 1), K. Nagaoka 1), M. Goto 1), J. Miyazawa 1), S. Masuzaki 1), N. Ashikawa 1), M. Yokoyama 1), S. Murakami 2), K. Narihara 1), I. Yamada 1), S. Kubo 1), T. Shimozuma 1), S. Inagaki 1), K. Tanaka 1), B.J. Peterson 1), K. Ida 1), O. Kaneko 1), A. Komori 1), and LHD Experimental Group 1)

1) National Institute for Fusion Science, Toki 509-5292, Japan
2) Department of Nuclear Engineering, Kyoto University, Kyoto 606-8501, Japan

e-mail contact of main author: takeiri@nifs.ac.jp

Abstract. High-Z plasmas have been produced with Ar- and/or Ne-gas fuelling to increase the ion temperature in the LHD plasmas heated with the high-energy negative-ion-based NBI. Although the electron heating is dominant in the high-energy NBI heating, the direct ion heating power is much enhanced effectively in low-density plasmas due to both an increase in the beam absorption (ionisation) power and a reduction of the ion density in the high-Z plasmas. Intensive Ne- and/or Ar-glow discharge cleaning works well to suppress dilution of the high-Z plasmas with the wall-absorbed hydrogen. As a result, the ion temperature increases with an increase in the ion heating power normalized by the ion density, and reaches 10 keV. An increase in the ion temperature is also observed with an addition of the centrally focused ECRH to the low-density and high-Z NBI plasma, suggesting improvement of the ion transport. The results obtained in the high-Z plasma experiments with the high-energy NBI heating indicate that an increase in the direct ion heating power and improvement of the ion transport are essential to the ion temperature rise, and that a high-ion temperature would be obtained as well in hydrogen plasmas with low-energy positive-NBI heating which is planed in near future in LHD.

1. Introduction

In the Large Helical Device (LHD), which is the world-largest superconducting helical device [1], it is quite important to investigate the confinement properties of high-ion temperature plasmas. Achievement of high temperature plasmas should also indicate the confinement ability of the high-energy ions. The high-electron temperature plasmas have been already achieved with centrally focused ECRH [2], and the improvement of electron confinement was observed due to suppression of the anomalous transport in the electron-ITB plasmas [3,4]. The LHD is equipped with three tangential negative-NB injectors in which the nominal injection energy of hydrogen beam is as high as 180 keV [5]. The LHD-NBI system was designed for achievement of high-$n\tau T$ plasmas and the injection energy was determined for the target density of $(3 – 5) \times 10^{19}$ m^{-3}. Against low-density hydrogen plasmas, then, most of the beam power goes to electrons due to the high injection energy and a large fraction of the injected neutral beam passes through the plasma without ionisation. As a result, the achieved ion temperature has been below 2 – 3 keV in hydrogen discharges using the negative-NBI [6]. There are two scenarios to raise the ion temperature in the LHD. One is to increase the direct ion heating power, and the other is to improve the ion transport. While plasma heating with low-energy positive-NBI systems would be effective to increase the ion-heating fraction so as in the present large tokamaks, we realized the enhancement of the ion heating power effectively by producing high-Z plasmas at low density [3,6,7]. The ion temperature was increased to 5 keV by Ne-gas puffing with an increase in the direct ion heating power [3,6]. However, dilution of the high-Z plasmas with hydrogen from the wall prevented the further increase in the ion temperature. We have performed the Ne- and/or Ar-glow discharge cleaning for reduction of the wall-absorbed hydrogen, and achieved the further increase in the ion temperature up to 10 keV with Ar-gas puffing. On the other hand, the transport

improvement is expected in the neoclassical electron root plasmas with positive radial-electric field [8], which was confirmed for electrons in the electron-ITB plasmas in the LHD with the centrally focused ECRH [3,4,9]. We have superposed the centrally focused ECRH to the high-Z NBI plasma as one approach to improve the ion transport, and observed an increase in the ion temperature. In the followings, we present the high-ion temperature experiments with the high-Z plasmas heated by the high-energy negative-NBI system in the LHD, with views of effectiveness of the high-Z glow discharge cleaning, plasma properties including high-energy ion behaviour in the high-Z discharges, and effect of the superposition of the ECRH to the high-Z NBI plasmas.

2. Negative-Ion-Based NBI system and ECRH system

The neutral beam injection (NBI) system in the LHD, which is characterized by high-energy NB injection produced through negative ions, consists of three tangential injectors, each of which has two large negative-ion sources [5,10]. One injector has the opposite injection direction to the other two injectors. The nominal injection energy is 180 keV and the beam species is hydrogen. The injection power has gradually increased year by year since the NBI system was operational in 1998, and reached 13 MW in the previous campaign. The achieved injection energy and power with one injector are 186 keV and 5.7 MW, respectively [11]. High-power neutral beams are injected usually for 2 sec with high reliability, and the injection duration can be extended over 100 sec with reduced power [12]. The shine-through beam, passing through the plasma without ionisation, is incident on the beam-facing armour tiles installed inside the LHD vacuum vessel. The shine-through power is estimated with a calorimeter array on the armour tiles, and the port-through injection power is determined with the shine-through power measurement [13].

The electron cyclotron resonance heating (ECRH) system employs 168GHz, 84GHz, and 82.7GHz gyrotrons, and each microwave is injected on the equatorial plane as a strongly focused Gaussian beam using vertical and horizontal antenna systems with quasi-optical mirrors [14]. In the experiments, the second-harmonic heating with two 82.7 GHz gyrotrons is utilized. The power deposition profile is estimated with ray tracing including a weakly relativistic effect.

3. Glow Discharge Cleaning with High-Z Gas

Since the ionisation cross-section for the injected beam is larger in the higher-Z plasmas, the beam absorption (ionisation) rate is increased especially for low-electron density plasmas in the high-Z discharges. Considering a reduced number of ions in the high-Z plasmas, the direct ion heating power is much enhanced even with the high-energy NBI heating. To realize such high-Z plasmas at low density the wall conditioning is important, because the high-Z plasmas should be diluted with the residual hydrogen during the discharge and a degree of the dilution be large in the low-density plasmas. For reduction of the wall-absorbed hydrogen intensive Ne- and/or Ar-glow discharge cleaning was performed. Figure 1(a) shows the ratio of the H_2 partial pressure to the total pressure before the start of the main discharges (after the glow discharge cleaning). In this case the high-Z experiments were made for three successive days (Jan. 13–15, 2004) and the Ne-glow discharge cleaning was performed for 64 hours prior to a series of the high-Z experiments. As shown in Fig. 1(a), the H_2 partial pressure after the high-Z glow discharge cleaning was much reduced compared with that after the H_2-glow discharge

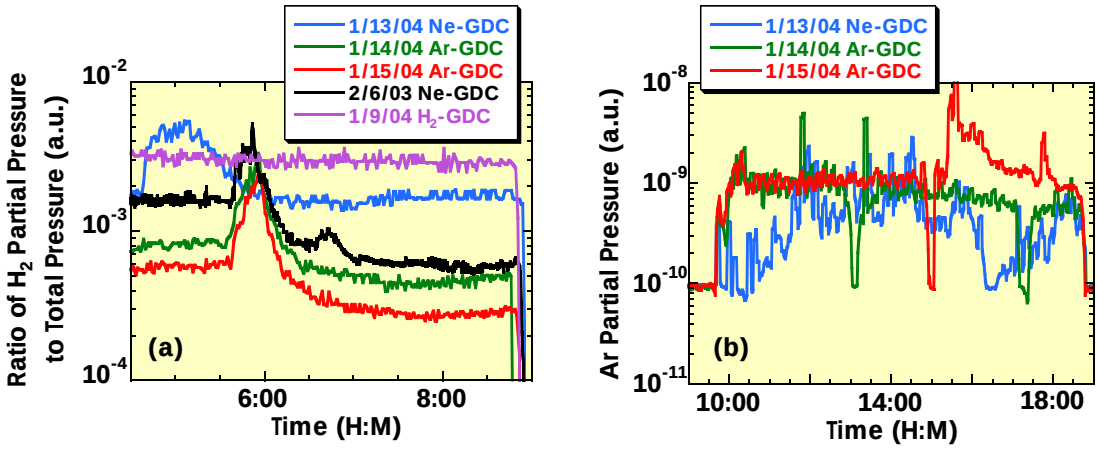

FIG. 1. (a) Ratio of the H_2 partial pressure to the total pressure after the glow discharge cleaning (before the start of the main discharges). Ti-gettering was applied after the Ne- or Ar-glow discharge cleaning and was not done after the H_2-one. (b) Ar partial pressure during the main discharges. The Ar gas was mainly puffed for the discharges. At around 15:00 on 1/15/04 the experiments were moved to high-density hydrogen discharges.

cleaning on the other day (Jan. 9, 2004). After the first-day experiment the Ar-glow discharge cleaning was applied during the successive two nights (Jan. 14 and 15, 2004). It is found that the H_2 partial pressure was reduced day by day, indicating reduction of the wall-absorbed hydrogen. It seems that the Ar-glow discharge cleaning is more effective for reduction of the H_2 partial pressure compared with the Ne-one (Feb. 6, 2003 is the successive third day of the Ne-glow discharge cleaning). The Ar partial pressure during the high-Z main discharges is shown in Fig. 1(b) for the three successive high-Z experiments (Jan. 13–15, 2004) in which the plasma was produced mainly with Ar gas-puffing. In the first day (Jan. 13) when the Ne-glow discharge cleaning was applied before the main discharges, the Ar partial pressure was gradually increased due to Ar gas-puffing in the main discharges, and it was decreased while the main discharge was suspended. In the second day (Jan. 14) when the Ar-glow discharge cleaning was applied, the Ar partial pressure showed a higher value than that in the first day, and it was slowly decreased as the main discharge progressed. The Ar partial pressure was maintained at a high value without a decrease in the third day (Jan. 15) when the second Ar-glow discharge cleaning was applied. After the high-Z experiments (around 15:00 on Jan. 15), the Ar partial pressure increased due to the following high-density H_2 discharge experiments. The successive two-nights of Ar-glow discharge cleaning should replace the wall-absorbed hydrogen with argon and be effective for the reduction of the residual hydrogen.

4. High-Ion Temperature in High-Z Discharges

4.1. Enhancement of Beam-Absorption Power

The ionisation (absorption) rate of the injected neutral beam is estimated with measurement of the shine-through power [13]. Figure 2 shows the ratio of the plasma absorption power to the port-through power of the injected neutral beams as a function of the line-averaged electron density. The beam absorption rate is fitted to $1-\exp(-\sigma_{\mathrm{eff}}\, n_e \ell)$ using the line-density $n_e \ell$, and, then, σ_{eff} represents the effective cross-section for the ionisation of neutral beam. In the figure, the absorption rates are plotted for two cases, the conventional hydrogen discharges and the Ne- or Ar-seeded discharges after the Ne-glow discharge cleaning. The plasma

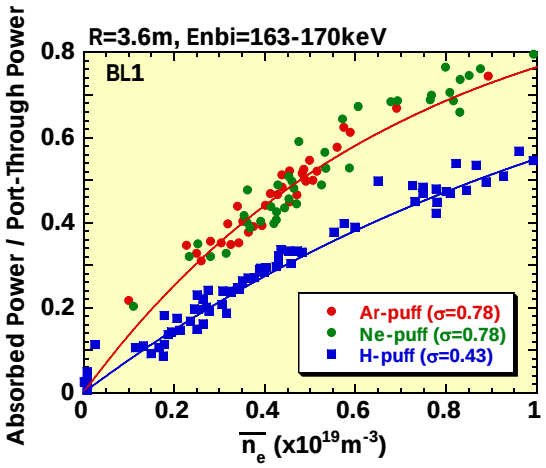

FIG. 2. Ratio of the plasma absorbed power to the port-through power of the injected neutral beams as a function of the line-averaged electron density for the Ar-, Ne-, and H_2-puffed plasmas. The injected beam energy ranges 163 – 170 keV. The data are fitted to 1-exp(-$\sigma n_e l$) using the line-density $n_e l$.

absorption power is enhanced in the Ne- or Ar-seeded plasmas compared with the H_2-puffed ones, and the effective cross-section for the beam ionisation is about 1.8 times larger. In low-electron density plasmas below $0.5\text{x}10^{19}\text{m}^{-3}$, the plasma absorption power is increased 1.6 times in the Ne- or Ar-seeded plasmas. Since the ion density is reduced compared with the electron density in the high-Z plasmas, the direct ion heating power is much enhanced. Consequently, with the high-Z discharges, the ion heating power by the high-energy NBI can be increased even in the low-density plasmas. In other words, with a view of the ion heating, the high-energy NBI heating in the high-Z plasmas is equivalent to the low-energy NBI heating in hydrogen discharges where the ion heating is dominant, although the plasma characteristics such as the collisionality are not the same. As shown in Fig. 2, the σ_{eff} is not so different between the Ne- and the Ar-seeded plasma. The σ_{eff} for the Ar-seeded plasma after the Ar-glow discharge cleaning also indicates nearly the same value as the Ne- or Ar-seeded plasma after the Ne-glow discharge cleaning.

4.2. Achievement of 10-keV Ion Temperature

Figure 3(a) shows the time evolutions of various plasma parameters in an Ar-puffed plasma after the Ar-glow discharge cleaning. After an increase in the electron density due to the Ar gas-puffing, the central ion temperature, measured with the Doppler broadening of an X-ray line of ArXVII, rapidly increases as the density decreases with an addition of another NBI power, and stays at high values. The ion temperature reaches 10 keV at around t=1.65s with an injection power of 12.2 MW, around 30 % of which is absorbed at an electron density of $0.37\text{x}10^{19}\text{m}^{-3}$. The electron temperature is also increased up to 4.6 keV, and, however, is much lower than the ion temperature. The observed beam slowing-down time after the NBI-off is as long as 1.2 sec probably due to both the low electron density and the high electron temperature, and the ion and electron temperatures show an extremely slow decay after the beam turn-off. The parallel beam-pressure should be large. The high-energy ion spectra measured with a Si-FNA detecting perpendicularly are shown in Fig. 3(b). At t=0.8-1.0s before the ion temperature rise, the high-energy ion spectrum is depressed less than 30 keV. On the other hand, no depression is observed on the spectrum at t=1.6-1.8s and the high-energy ion flux is increased when the ion temperature rises to 10 keV, indicating that the injected high-energy particles are slowing-down to the thermal energy without large loss. As shown in Fig. 3(c), the density profile becomes peaked (t=1.64s) with a reduction of the density in outer plasma region at around ρ=0.8 as the ion temperature increases, compared with that before the temperature increase (t=0.88s) showing hollow or flat profiles.

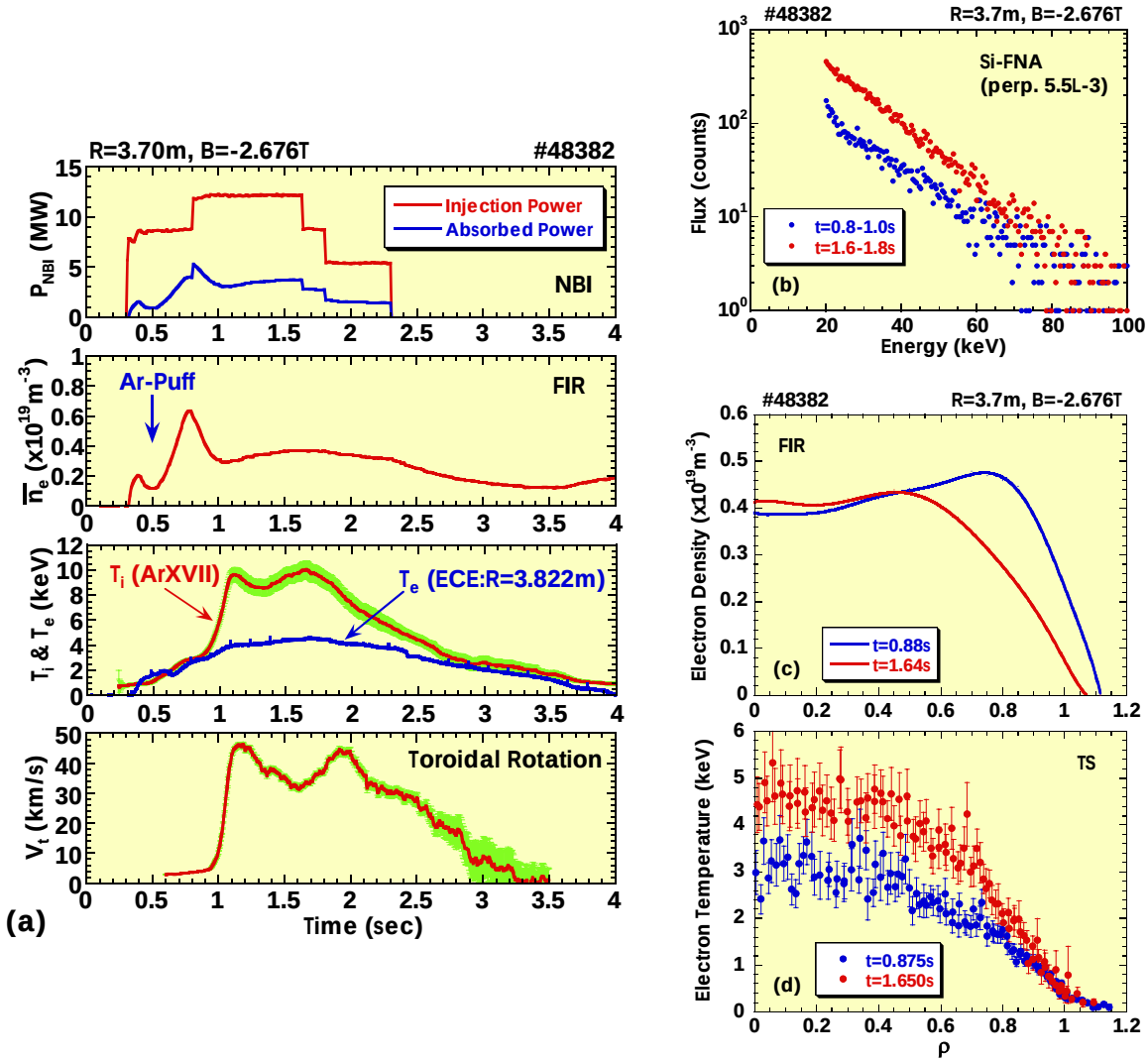

FIG. 3. (a) Time evolutions of the injection and absorption powers, the line-averaged electron density, the ion and electron temperatures, and the toroidal rotation velocity (from the top). (b) High-energy ion spectra measured with a perpendicularly detected Si-FNA. The fluxes are plotted as integrated counts for t=0.8-1.0s and t=1.6-1.8s. (c) Electron density and (d) electron temperature profiles at t=0.88s and t=1.65s.

Corresponding to the density peaking, the electron temperature profile shows a steep gradient at around ρ=0.8, as shown in Fig. 3(d). Theoretical calculation of neoclassical ambipolar flux considering multi-ion species indicates generation of a strong positive radial-electric field at around ρ=0.8, suggesting a confinement improvement there. A large toroidal rotation is observed corresponding to an increase in the ion temperature as shown in Fig. 1(a), and the toroidal rotation velocity reaches 46 km/s, which is about 30 % of the Ar-thermal velocity, suggesting also a confinement improvement in the high-ion temperature plasmas with the high-Z discharge.

4.3. Properties of High-Z and High-Ion Temperature Plasmas

It is important to clarify the properties of high-Z and high-ion temperature plasmas. From a measurement of the recombination Hα intensity at the plasma termination, the H ion density is roughly estimated to be 25 – 40 % of the electron density, and this ratio is not so changed

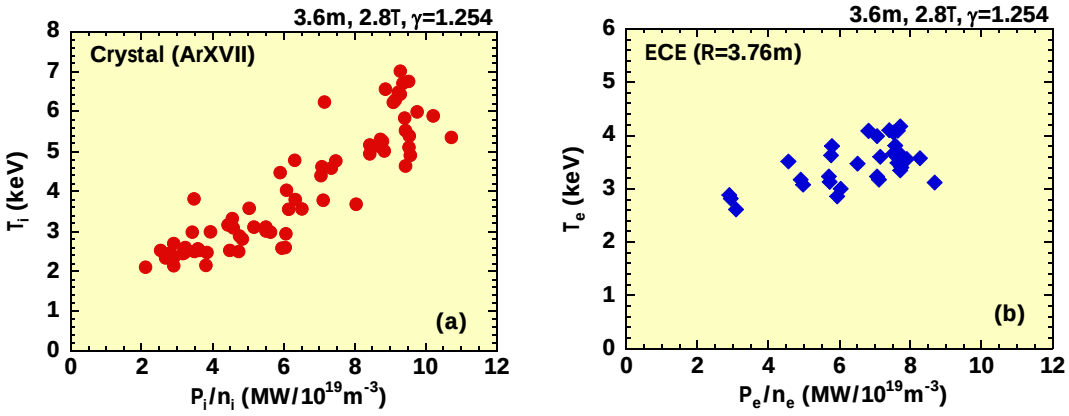

FIG. 4. (a) Ion temperature as a function of the ion heating power normalized by the ion density. (b) Electron temperature as a function of the electron heating power normalized by the electron density. The Ne or Ar gas is puffed and intensive Ne-glow discharge cleaning was applied for a series of high-Z experiments. The magnetic axis position is 3.6m.

in a series of low-density and high-Z discharges. Thus, the H ions seem to dominate the species number ratio even in the high-Z plasmas. The Z_{eff} is around 7 and around 12 if the other ion species is Ne alone and Ar alone, respectively. Although the other possible impurity is C in the LHD with carbon divertors, the Z_{eff} is thought to range 7 – 12 in the Ne and Ar discharges, and the total ion density should be 30 – 46 % of the electron density. Then, the ion heating power is around a third of the NBI-absorption power. Here, we can estimate the ion heating power normalized by the ion density. Compared with the hydrogen discharges, the normalized ion heating power is much enhanced by a factor of 4 - 5 in the high-Z and low-density plasmas by both an increase in the beam absorption power and a reduction of the ion density. Figure 4(a) shows the ion temperature as a function of the normalized ion heating power for the Ar- and Ne-puffed plasmas after the Ne-glow discharge cleaning. It is found that the ion temperature is increased with an increase in the normalized ion heating power in the Ar- and Ne-puffed plasmas and that no distinct saturation of the increase in the ion temperature has been observed. The electron temperature as a function of the electron heating power normalized by the electron density is also shown in Fig. 4(b). The electron temperatures for the normalized heating power show similar values to the ion temperatures although the dependency is not so clear due to a narrower power range. It seems that the ion and electron temperatures are increased with increases in the direct ion and electron heating powers, respectively. Since the collisionalities of high-Z and H ions are considered to be in plateau regime, the dependence of the ion temperature is not directly applied to the hydrogen discharges in collisionless regime. However, the experimental results obtained in the high-Z discharges indicate that there is a possibility to achieve a high-ion temperature as well in hydrogen discharges if the direct ion heating power is increased to the same power density as that in the high-Z discharges.

Assuming that the ionised hydrogen particles of 180keV – 3MW are confined for 1 sec, corresponding to the beam slowing-down time, the hydrogen ion density deriving from the injected beam is 0.35 x 10^{19} m^{-3}. Therefore, it is considered that the hydrogen ions in the high-Z discharges are mainly supplied from the injected beam. In other words, it would be difficult to realize the further high-Z discharges with the NBI heating.

4.4. Ion Temperature Rise with Superposition of ECRH

When centrally focused ECRH is superposed on the NBI plasmas, improvement of the electron transport was observed in LHD. This improvement is correlated with realization of the electron root where the positive radial-electric field is generated due to neoclassical ambipolar flux [3,4,8,9]. However, no definite increase in the ion temperature has been observed, probably because the ion heating power is too small in low-density hydrogen plasmas due to the high injection energy. Figure 5(a) shows the comparison between the NBI-only plasma and the NBI+ECRH plasma in low-density and Ne-puffed discharges after the Ar-glow discharge cleaning. By the superposition of the ECRH of 470 kW the electron temperature is much increased to 3 keV from 2 keV, and accordingly the ion temperature is also increased by a factor of 1.5. Note that the integration time of the T_i measurement is 150 – 300 ms. Since the electron-ion heat exchange time is as long as a few seconds for Ne, Ar, or H ions and an increase in the ion heating ratio by the electron temperature rise is as small as about 10 %, it is suggested that the ion temperature increase is due to an improvement of the ion transport. Comparison of the electron density and temperature profiles between the NBI-only plasma and the NBI+ECRH plasma is shown in Figs. 5(b) and (c), respectively. As shown in Fig. 5(c), with the superposition of the ECRH the electron temperature profile forms a steep gradient at ρ=0.4-0.6, just outside of the injection region of the focused ECRH at around ρ=0.3. As the neoclassical calculation of the ambipolar flux considering multi-ion species shows generation of a positive radial-electric field in a region outside around ρ=0.4 with the superposition of the ECRH, there is a possibility of improvement of the ion transport in the electron root. Although the density profile usually becomes hollow with applying the ECRH, it becomes peaked with a reduction of outer region density in the NBI+ECRH plasma

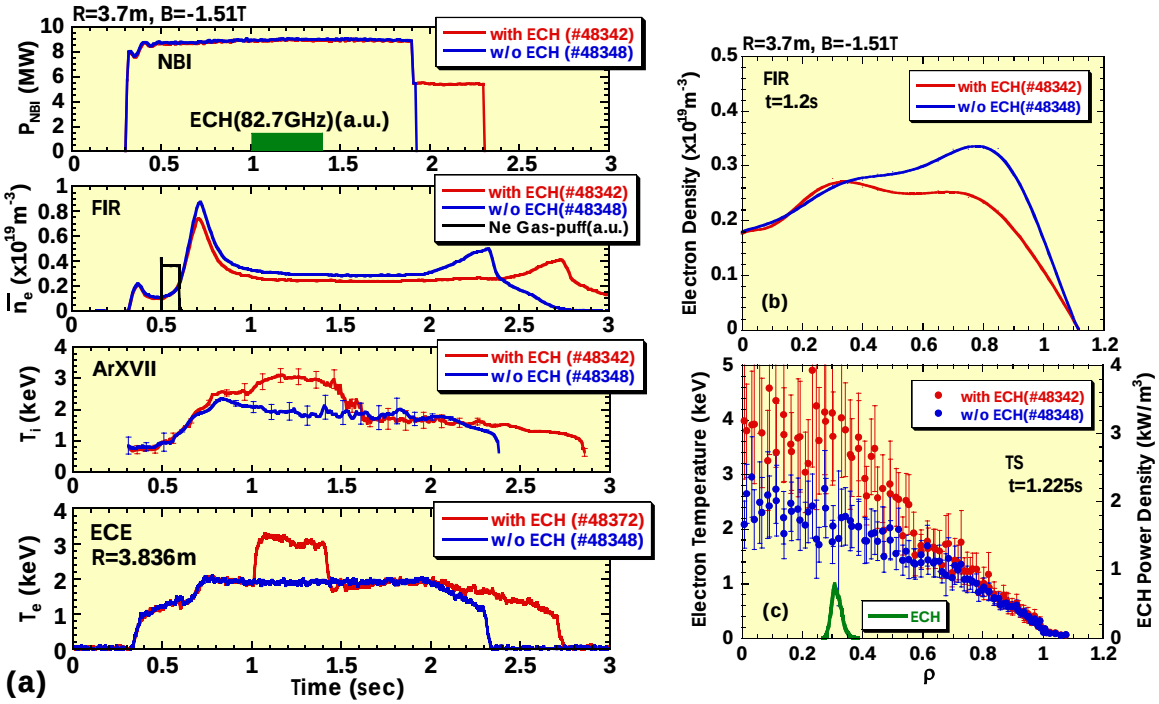

FIG. 5. (a) Time evolutions of the NB injection powers and the ECRH timings, the line-averaged electron densities, the ion temperatures, and the electron temperatures (from the top), for the NBI-only plasma and the NBI+ECRH plasma of the Ne-puffed discharges. (b) Electron density and (c) electron temperature profiles at t=1.2s for the NBI-only and the NBI+ECRH plasmas. The ECRH power deposition profile is also indicated in (c). The magnetic axis position is 3.7m.

with a rise in the ion temperature, as shown in Fig. 5(b). The correlation of the increase in the ion temperature and the density peaking is recognized in the high-Z plasmas including the impurity pellet injection, and the particle transport would be changed in the high-Z plasmas with high-ion temperature.

5. Concluding Remarks

The high-Z discharges are utilized for high-ion temperature experiments with high-energy negative-ion-based NBI heating, in which the electron heating is dominant usually in hydrogen discharges. In the high-Z plasmas the beam absorption (ionisation) rate is increased and the plasma ion density is reduced, resulting in much enhancement of the effective ion heating power by a factor of 4 – 5. The ion temperature is increased with an increase in the ion heating power normalized by the ion density, and reaches 10 keV in an Ar-seeded discharge. In the high-ion temperature plasmas realized in the high-Z discharges, there are observations suggesting transport improvement. The toroidal rotation velocity is increased corresponding to the increase in the ion temperature, and the density profile becomes peaked with a reduction of outer density at around ρ=0.8, where the electron temperature gradient becomes steep with a theoretical calculation result of generation of a strong positive radial-electric field. Intensive Ar- and/or Ne-glow discharge cleaning is effective to reduction of the wall-absorbed hydrogen with which the high-Z plasmas are diluted. With superposition of the centrally focused ECRH on the NBI-heated high-Z plasma, an increase in the ion temperature is observed, suggesting improvement of the ion transport in the neoclassical electron root.

Two scenarios for increasing the ion temperature, i.e., to increase in the direct ion heating power and to improve the ion transport, are experimentally demonstrated with high-Z plasmas in LHD. The high-Z plasmas heated by high-energy negative-NBI is equivalent to the hydrogen plasmas heated by low-energy positive-NBI in that the effective ion heating power is large, although the plasma parameters such as collisionality are not necessarily the same. The positive-NBI heating, which is planed in near future in LHD, could demonstrate to increase the ion temperature in hydrogen discharges.

References

[1] O. Motojima, *et al.*, Phys. Plasmas **6** (1999) 1843.
[2] S. Kubo, *et al.*, Proc. 19th IAEA Fusion Energy Conf., Lyon, 2002, EX/C4-5Rb.
[3] Y. Takeiri, *et al.*, Phys. Plasmas **10** (2003) 1788.
[4] T. Shimozuma, *et al.*, Plasma Phys. Control. Fusion **45** (2003) 1183.
[5] O. Kaneko, *et al.*, Nucl. Fusion **43** (2003) 692.
[6] S. Morita, *et al.*, Nucl. Fusion **43** (2003) 899.
[7] Y. Takeiri, *et al.*, Proc. 30th EPS Conf., St. Petersburg, 2003, P-2.171.
[8] M. Yokoyama, *et al.*, Nucl. Fusion **42** (2002) 143.
[9] K. Ida, *et al.*, Phys. Rev. Let. **91** (2003) 085003.
[10] Y. Takeiri, *et al.*, Rev. Sci. Instrum. **71** (2000) 1225.
[11] K. Tsumori, *et al.*, this Conference, FT/1-2Rb.
[12] Y. Takeiri, *et al.*, Plasma Phys. Control. Fusion **42** (2000) 147.
[13] M. Osakabe, *et al.*, Rev. Sci. Instrum. **72** (2001) 586.
[14] T. Shimozuma, *et al.*, Fusion Eng. Design **53** (2001) 525.